Experimental study on the shear strength and failure mechanism of mountain glacier ice

Minggao Tang[1,2], Huanle Zhao[1,2,*], Qiang Xu[1,2], Wentao Ni[3], Guang Li[1,2], Zhiping Zuo[1,2], Xu Chen[1,2], Yihua Zhong[4]

[1]State Key Laboratory of Geohazard Prevention and Geoenvironment Protection, Chengdu University of Technology, Chengdu, 610059, China
[2]College of Environment and Civil Engineering, Chengdu University of Technology, Chengdu, 610059, China
[3]Sichuan Natural Resources Survey and Design Group Co., Ltd., Chengdu, 610051, China
[4]Institute for Disaster Management and Reconstruction, Sichuan University, Chengdu 610200, China

Correspondence: Huanle Zhao (2020010067@stu.cdut.edu.cn)

Abstract. As global warming increases the frequency of ice avalanches, understanding the mechanical behavior of mountain glacier ice becomes critical. Through more than 250 field and laboratory tests, the variations of four kinds of glacier media with temperature and debris content were analyzed. The four types of glacial media are polycrystalline ice, ice-rock composite, fine debris ice, and coarse debris ice. Our comprehensive analysis reveals a positive correlation between ice density and debris content, but with a notable nonlinear decrease in porosity as debris content escalates. All types of ice have strain-softening characteristics in the shearing process. Shear strength is significantly modulated by debris content and temperature gradients. Fine debris ice exhibits the highest strength, followed by coarse debris ice, polycrystalline ice, and ice–rock composite. Polycrystalline ice displays the strength of nonlinear degradation with increasing temperature and ice–rock composite shows the strength of linear degradation with increasing temperature. Fine and coarse debris ice display the strength of the nonlinear enhancements with increasing debris content. The mechanism by which the strength of polycrystalline ice and ice-rock composites decreases with temperature increases is discussed. The strength enhancement of debris ice caused by increased debris content is expounded. It is believed that the emergence of liquid water is one of the reasons for the strength degradation. The solid particle effects (biting, friction, and crushing) are essential reasons for strength enhancement. This study addresses the research gap in mountain glacier ice mechanics driven by global warming, a previously underexplored subject. This investigation expounds on the nuanced interdependencies between temperature and debris content in determining glacier ice' shear strength, paving the way for force avalanche prediction models and disaster prevention strategies. It provides pivotal insights into mountain glacier ice behavior under different environmental conditions.
Keywords. Geological hazards; Glacier ice; Ice avalanche; Shear strength; Mechanism; Temperature; Debris content

1 Introduction

30

avalanches (IAs) have increased in frequency over the past decade (Zhang et al., 2024) and caused severe losses of life and property, such as the Aru IA killed nine herders and hundreds of their animals (Tian et al., 2017; Kääb et al., 2018). The Sedongpu IA temporarily blocked the Yarlung Tsangpo river (Zhao et al., 2022). The Chamoli ice-rock avalanche damaged two hydropower plants, and more than 200 people were killed or are missing (Shugar et al., 2021). 11 mountaineers were

35 killed and 7 others were injured by Marmolada IA (Bondesan et al. 2023). The Sixth Assessment Report Climate Change 2023 shows that the global temperature increase is expected to reach 1.5 °C between 2021 and 2040 (IPCC, 2023). The instability of numerous glaciers in the world due to global warming threatens the safety of people's lives and property. Tang et al. (2023) identified 581 IAs on the Tibetan Plateau (TP). In the Himalayas, several million natives can be affected by IAs (Dubey et al., 2023). The stability of the glacier is closely related to the changes in glacier ice shear strength. The study of

40 shear strength and failure mechanism of glacier ice is of great scientific value in revealing the mechanism and prevention of IAs.

Systematic consideration of material composition and contact relationships reveals that the main failure surface (band) of ice avalanche (including ice-rock avalanche) can occur in ice (Bondesan et al. 2023), debris ice (Gilbert et al., 2018), ice-rock interface (Li et al., 2024), the ice debris–rock interface and within the subglacial rock (Shugar et al. 2021). Here we

45 collectively refer to the glacial medium. Whether they fail or not depends on the strength value (Fitzsimons et al. (2024)). This value is very important in the process of glacier stability evaluation (e.g., Gilbert et al., 2018; Wei et al., 2024), similar to the need for slope stability evaluation. Temperature and debris content are important factors affecting its strength. Exploring and establishing the relationship between these factors and the medium strength of mountain glaciers is the basis of glacier stability evaluation, which needs a series of experimental data as support. Before this, studies on the effect of

50 temperature on ice strength have been carried out continuously (e.g. Xu et al., (2011); Ji et al., (2013); Guo and Meng, (2015); Farid et al., 2017; Shan et al., 2018; Zhang et al., 2022), but the focus is not on glacial ice. The study of the ice-rock interface is also limited to the frost heave failure of the freeze-cracked rock mass (Su et al. (2024)) or the deterioration of the freeze-thaw cycle. There are also relatively few studies on the effect of debris content on the strength of debris-ice mixtures (Nickling and Bennett (1984); Moore (2014); Huang et al. (2023a)). Importantly, Fish and Zaretsky (1997) collected part of

55 the existing research and test data and established the relationship between ice strength and temperature. Fu et al. (2021) established the relationship of shear strength degradation of moraine under thawing conditions through laboratory experiments. Huang's team established the degradation relationship of ice-rich debris shear strength under ice melting conditions through laboratory experiments (Huang et al. (2023a)), and the relationship of ice-rich debris-rock interface shear strength considering fluctuation, temperature, stress, and ice content (Huang et al. (2023b); Meng et al. (2024)). Nickling and

60 Bennett (1984) tested the shear strength of frozen coarse debris with varying ice content and discussed the relationship between them. Moore (2014) investigated the effect of debris volume fraction on the strength or creep stress of the debris ice mixture by normalizing test data from different sources. Fitzsimons et al. (2024) compared the strength of clean ice,

laminated ice, and massive ice in glaciers in the field and the lab. To promote the application of glacier stability evaluation, it is necessary to systematically study and discuss the strength of the glacial medium, especially in the climate-sensitive region
65   of the High Asian Mountains.

Mountain glacier ice, with its unique formation process, structure, and composition, particularly due to the incorporation of bedrock powder (Moore, 2014), has not been thoroughly investigated. This gap in the literature has left the mechanisms of mountain ice largely unexplored, which are pivotal to understanding the initiation and propagation of IAs. Addressing this deficit, our study examines glacier ice from Gongga Mountain, which has not been extensively studied in terms of glacier ice
70   mechanics. Based on field testing, we have conducted over 250 direct shear tests in a controlled laboratory setting. These tests scrutinize the behavior of glacier ice with different temperatures (-0.5 to -40 °C) and debris contents (fine debris at 10-30% and coarse debris at 20-60%). Our primary goal is to decipher the shear strength characteristics of mountain glacier ice. We also aim to shed light on the mechanical disparities between glacier ice and other types of ice and deepen our understanding of glacier ice's distinctive properties. These findings are to contribute significantly to the theoretical
75   understanding of IA mechanisms. The results will aid in developing effective disaster prevention strategies and address critical geotechnical engineering and environmental management needs.

2 Study object and method

2.1 Study object

The important factors in studying IAs are the material composition of glacier ice and the contact relationship with the ice bed.
80   Moore, (2014) classified glacial material based on rock and debris content into clean ice, dirty ice, very dirty ice, ice-rich debris, and ice-poor debris. Vivian, (1980) distinguished two types of ice-bed contact relationships: the ice is in direct contact with the bed, and some cavities exist between the ice and the rock. For this reason, we selected the Gongga Glacier for field investigation and testing (Fig. 1). The Gongga Glacier is a warm mountain glacier located in Kangding City, Ganzi Tibetan Autonomous Prefecture, Sichuan Province. The geographical coordinates are 101°41′25″E, 29°17′37″N. The main
85   peak of Gongga Mountain is 7,508.9 meters above sea level, which is the highest peak in Sichuan Province. It is known as the "King of Shu Mountain" and is one of the mountains with the largest height difference in the world. According to the field survey, the terminus structure from top to bottom consists of an ice layer, a fine debris-ice layer, and a coarse debris-ice layer (Fig. 1c). The ice is in direct contact with the bed at a higher position (Fig.1b). Therefore, we are considering the material compositions of polycrystalline ice, debris ice (fine debris ice and coarse debris ice), and the direct contact
90   relationship between ice and rock.
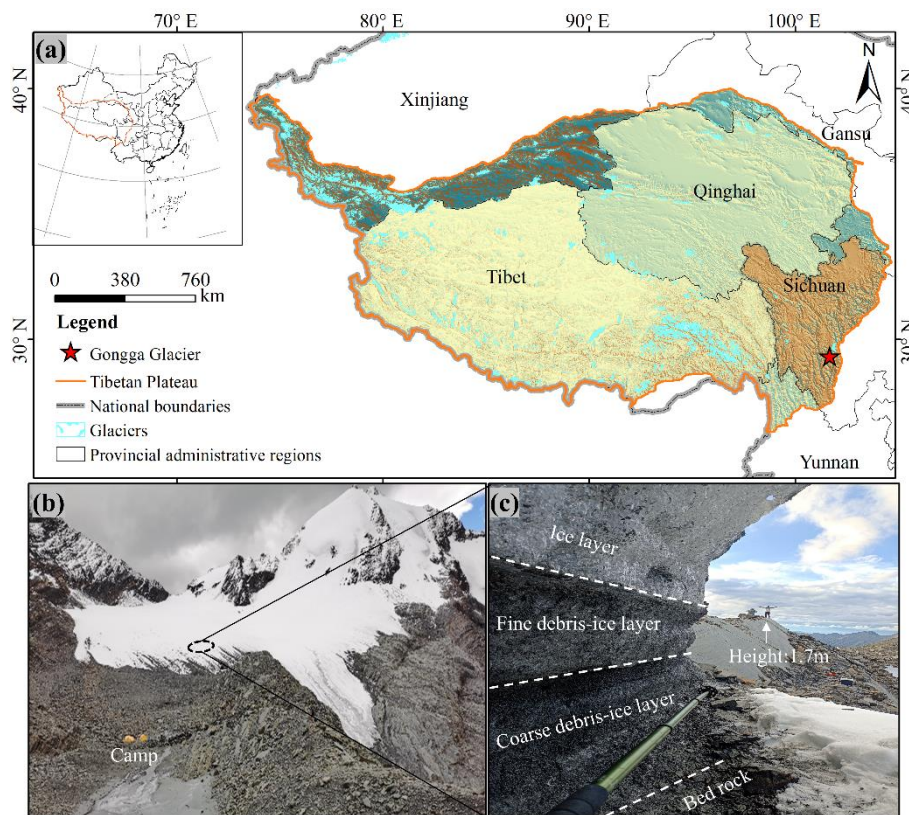
Figure 1. Study object. **(a)** Geographical location. **(b)** Gongga Glacier. **(c)** The structure of the glacier.

2.2 Sample control conditions

We collected 19 samples at the glacier terminus (Fig. 1) for physical parameter tests: polycrystalline ice (3 samples), fine
95 debris ice (3 samples), and coarse debris ice (3 samples). We tested the shear strength of polycrystalline ice at different
normal stresses: 100 kPa (2 samples), 200 kPa (2 samples), 300 kPa (2 samples), 400 kPa (2 samples), and 500 kPa (2
samples). The results of the fundamental physical properties are shown in Table 1.

Table 1. Field test data.

Site	Test items	Value
Gongga Glacier	Ice temperature	-0.5 ℃
	Debris type	Slate
	Fine debris content	11%
	Fine debris size	< 5 mm
	Coarse debris content	23%
	Coarse debris size	5~10 mm

100 The density of the sample was measured using the Archimedes drainage method. Porosity was calculated using Eq. (1):

$$e = \Delta V / V ,\qquad\qquad\qquad (1)$$

Where e is the porosity, ΔV is the volume change formed by the sample in the measuring cup before and after melting (use it as an estimate of the pore volume), and V is the sample volume (when measuring, the sample needs to be wrapped with a small amount of tin foil, and the volume of the tin foil is ignored here); It should be emphasized that the density and porosity

105 mentioned in the article were measured values before the test.

The shear strength was tested in the field using a portable direct-shear test instrument. An electric saw was used to create samples with dimensions of $50 \times 50 \times 50$ mm for the test. The steps involved in the test were as follows: sample production, commissioning equipment, sample installation, and sample testing (Fig. 2). Based on the field testing results, the laboratory sample's shear strength and physical properties have been controlled to make them more representative of glacier ice.
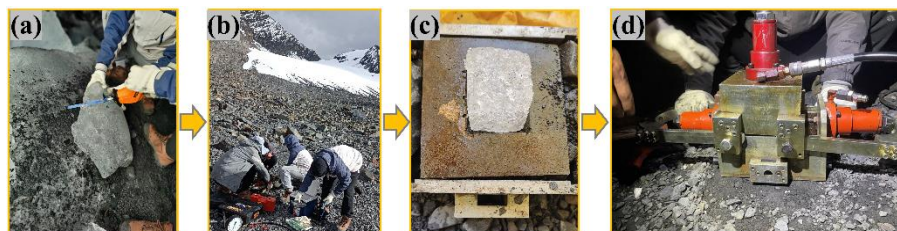
110

Figure 2. Field test steps. **(a)** Sample production. **(b)** Commissioning equipment. **(c)** Sample installation. **(d)** Sample testing.

2.3 Sample preparation

The laboratory sample preparation was divided into two stages (Figs. 3A and 3B): **(1)** Making ice. Fill an expanded polystyrene (EPS) box with water, put it in a low-temperature box (Fig. 3a), freeze it into ice cubes, and then use an ice

115 crusher to crush the ice cubes to a particle size of 2 mm for later use (Fig. 3b). **(2)** Making samples. The samples with a size of $50 \times 50 \times 50$ mm were made and divided into polycrystalline ice, debris ice, and ice–rock composite samples (Fig. 3d). The representative rock type on the TP is gneiss (Tang et al., 2022). **1)** When making polycrystalline ice samples, use the isostatic pressing method (Geotechnical Test Method Standard, Page 10) of two layers (each layer is 25 mm) to create the initial shape. Then, it is placed into a low-temperature box for preconsolidation pressure freezing (Fig. 3c) to achieve the

120 final shape (Fig. 3d). **2)** To ensure sample uniformity, thoroughly mix the debris and broken ice, following the sample preparation method for coarse-grained soil in the Geotechnical Test Method Standard. The two-layer isostatic pressing was also used to create the initial shape. Specifically, debris (consisting of fine debris and coarse debris) was obtained through the screening method. The sieves used were sized 5 and 10 mm, based on the particle size of the fine debris (less than 5 mm) and the coarse debris (5–10 mm) obtained from the field survey. **3)** When making ice-rock composite samples, place the cut

125 flat and saturated rock block into the lower portion of the sample container, which is bounded by half of the container's height. The upper portion should be filled with crushed ice, forming the initial shape using isostatic pressing.
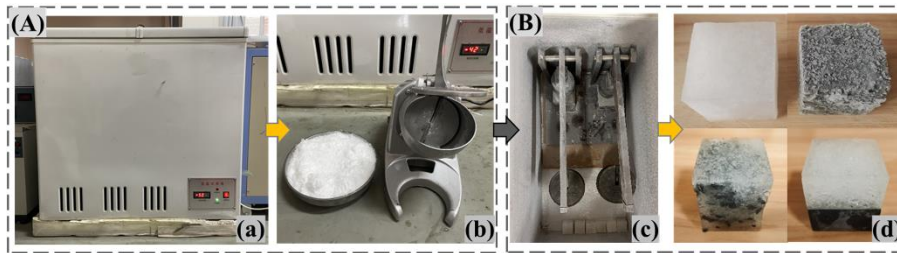
Figure 3. Sample preparation steps for laboratory. **(A)** Making ice (**(a)** Frozen ice cubes and **(b)** Broken ice) and **(B)** Making samples (**(c)** Preconsolidation pressure frozen and **(d)** Finished samples).

130   Due to the pressure needed during glacier formation in the field, the initially shaped sample required preconsolidation before being used as a test sample. The sample loaded into the container was compacted with a self-designed instrument (Fig. 3c). The pressure was converted using Eq. (2), and the additional weight of the scale weights was calculated using the lever principle. Field glacier parameters with a density of 0.85 g/cm^3 and a depth of 30 m were used here. The samples could be shaped (Fig. 3d) after being compacted for 24 hours (Geotechnical Test Method Standard, Page 87) in a low-temperature

135   environment. The target temperatures are -0.5, -10, -20, -30, and -40 °C.

$$P = \rho g h = F / A = mg / A ,$$ (2)

Where P is the self-weight stress, ρ is the field glacier ice density, g is the acceleration of gravity, h is the thickness of the glacier, F is the pressure in a laboratory sample, A is the cross-sectional area of the laboratory sample, and m is the mass of weight. It can be calculated that a force of 0.625 KN is required to apply a consolidation stress of 250 kPa, and a weight of

140   62.5 kg needs to be applied to the sample (the final weight mass is converted through the lever principle).

2.4 Laboratory test scheme

We designed laboratory samples as polycrystalline ice, ice-rock composite, and fine and coarse debris ice, with normal stress, temperature (ice temperature, the temperature involved below is also the same), and debris content as control variables (Table 2). The contents of fine and coarse debris ice were determined based on the field investigation results, taking into

145   account that the coarse debris ice layer in the glacier is deposited beneath the fine debris ice layer, and the debris content is naturally abundant. Furthermore, if the fine debris exceeds 30% during sample preparation, it becomes difficult to shape the sample.

150

Table 2. Laboratory sample and test scheme.

Sample name	Sample number	Normal stress (kPa)	Temperature (°C)	Debris content (mass ratio, %)
Polycrystalline ice	B-		-0.5, -10, -20, -30, -40	0
Ice–rock composite	B-Y-	100, 200, 300, 400, 500	-0.5, -10, -20, -30, -40	0
Fine debris ice	Y-		-20	10, 15, 20, 25, 30
Coarse debris ice	S-		-20	20, 30, 40, 50, 60

The YDS-2 type multifunctional tester was used for laboratory experiments (Fig. 4). This tester had a maximum vertical pressure of 500 KN and a maximum horizontal pressure of 300 KN, with a maximum travel distance of 60 mm. The experimental steps were as follows: **(1)** Ensure that the YDS-2 tester is positioned next to the low-temperature box. The purpose is to minimize the exposure time of the sample to the environment, preventing significant temperature changes. **(2)** Liquid nitrogen (-196.56 °C) was used to gradually cool the tester (upper and lower shear box, transmission block (Fig. 4) until it reached the same temperature as the target temperature sample. Remove the target temperature sample from the low-temperature box and place it into the shear box. **(3)** In the data collection instrument software, the force was set to 0. We pressurized the vertical pressure device using the oil pump, maintained a predetermined pressure, and zeroed the displacemen. **(4)** Use the fast shear method to shear the sample, ensuring that the sample is destroyed within 3-5 minutes (refer to Geotechnical Test Method Standard, Page 124), and click to collect data automatically at the same time. **(5)** Data recording was stopped after shearing. To ensure the representativeness of the failure mode, the shear box is lifted out as a whole. The shear box is carefully removed by hand to avoid direct contact with the damaged sample, and the failure mode of the shear surface is photographed and recorded. A portable shear tester of the XJ-2 type, similar to an indoor experimental instrument but lighter, was used in field experiments. The only difference was the absence of automatic collection instruments.
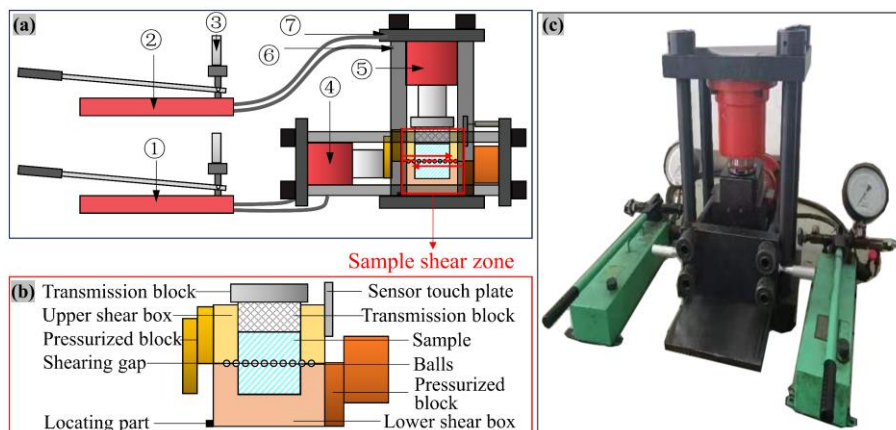
175   **Figure 4** YDS-2 rock and soil mechanics properties multifunctional testing instrument. **(a)** Structure of instrument (① Axial force loading pump. ② Shear force loading pump. ③ Pressure gauge. ④ Shear force jack. ⑤ Axial force jack. ⑥ Inlet pipe. ⑦ Outlet pipe). **(b)** Detail. **(c)** Photograph of instrument.

3 Results

3.1 Physical properties of mountain glacier ice

180   Table 3 compares the physical parameters of polycrystalline ice at -0.5°C in the field and the laboratory. The density of polycrystalline ice in the field and the laboratory was less than 1 g/cm³ (This falls within the glacier ice density range: 0.830-0.923 g/cm³ (Cuffey and Paterson, 2010)) with minor porosity. The error in the physical parameters of polycrystalline ice in the laboratory and the field was within 5% (Kutliyarov et al. 2020), indicating that the laboratory ice samples were congruent with the field ice samples.

185   **Table 3.** Comparison of the physical parameters of field and laboratory polycrystalline ice

Index	Gongga Glacier ice	Laboratory polycrystalline ice	Error (%)
Temperature (℃)	-0.5	-0.5	0.0
Density (g/cm³)	0.856	0.854	-0.2
Porosity	0.122	0.123	0.8

The relationship curves between the density, porosity, and debris contents of glacier ice at -20 °C are shown in Fig. 5. Fig. 5a represents the increase in fine debris content, and Fig. 5b represents the increase in coarse debris content. As the graph shows, the density is positively correlated with both types of debris content, which are in the ranges of 0.8–1.4 g/cm³ and

190   0.8–2.0 g/cm³ for fine and coarse debris, respectively. As the debris content increases, the porosity exhibits a nonlinear decreasing trend, ranging between 0.06 and 0.14.
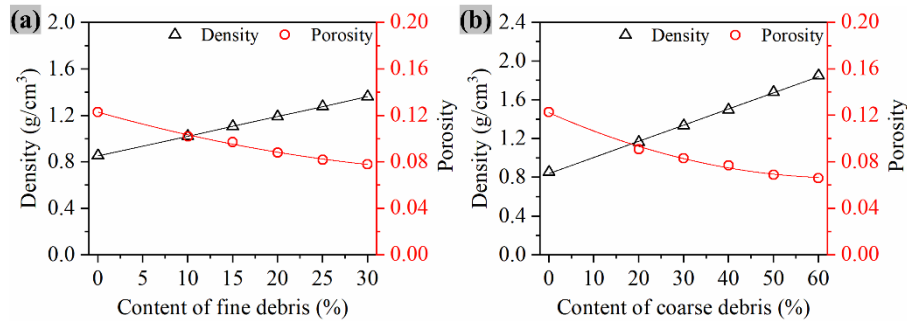
Figure 5. Debris content–density and debris content–porosity curves. **(a)** Variations in the physical parameters of fine debris ice and **(b)** Variations in the physical parameters of coarse debris ice.

3.2 Shear stress–displacement curves of mountain glacier ice

3.2.1 Shear stress–displacement curves considering different temperatures

The shear stress-shear displacement relationship for polycrystalline ice subjected to normal stress of 200 kPa is depicted in Fig. 6a. As the shearing process unfolds, the shear stress-shear displacement curve exhibits a parabolic descent beyond its peak value, signifying a phenomenon of strain softening. Literature suggests that elevated temperatures result in a decrease in the strength of ice crystal structures (Fan, 2021), thereby reducing their ability to resist deformation. The peak stress diminishes from 307 to 170 kPa, accompanied by a decrease in the shear displacement necessary to attain said peak stress. When the temperature is close to 0 °C, the sample tends to melt, and the liquid water (Cuffey and Paterson, 2010) lubrication and softening interface significantly reduce shear stress. The laboratory test curve of the ice-rock composite sample is shown in Fig. 6b. This graph illustrates the strain-softening characteristics during the shearing process. The ice-rock composite sample was shaped through the preconsolidation pressure freezing of ice and rock. The strength at the interface is weak.

When synthesizing the shear stress-displacement curves for polycrystalline ice and the ice-rock composite, the trends were as follows: both shearing processes exhibit strain-softening characteristics. The peak shear stress decays as the temperature increases (polycrystalline ice from 307 to 170 kPa; ice-rock composite from 286 to 136 kPa).
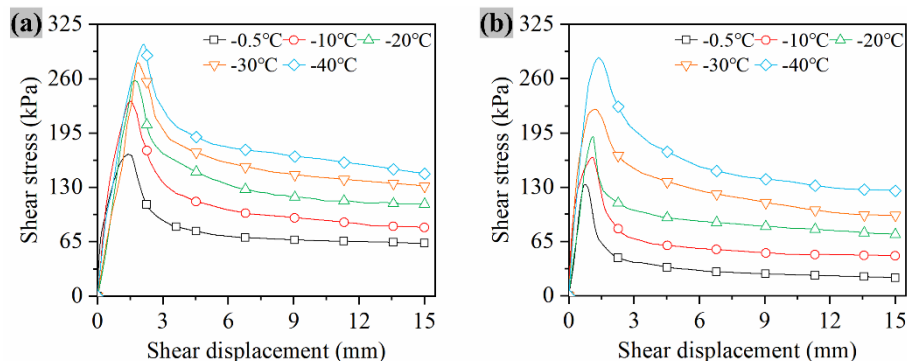
Figure 6. Shear stress–displacement curves at different temperatures (normal stress of 200 kPa). **(a)** Shear stress–displacement curve of polycrystalline ice and **(b)** Shear stress–displacement curve of the ice–rock composite.

3.2.2 Shear stress-displacement curves for different debris contents

Shear stress-shear displacement curves for fine and coarse debris ice are shown in Fig. 7. Both exhibit strain-softening characteristics during the shearing process. The characteristics depend on the fracture of the ice body on the shear plane and

215 the dislocation of debris. The slope of the pre-peak curve changes slightly as the debris content increases, indicating structural strengthening. Increased fine debris content can cause the sample's peak shear stress to increase more than increased coarse debris content (fine debris ice 20%, 368 kPa / 30%, 468 kPa; coarse debris ice 20%, 309 kPa / 30%, 369 kPa). Fine debris has a larger specific surface area than coarse debris, which increases the contact between debris, forms skeleton stress, and enhances the ability to resist deformation. Increasing the debris content increases the peak shear stress,

220 with fine debris ice increasing from 260 to 468 kPa and coarse debris ice increasing from 260 to 580 kPa. Additionally, it also increases the shear displacement required to reach peak stress.
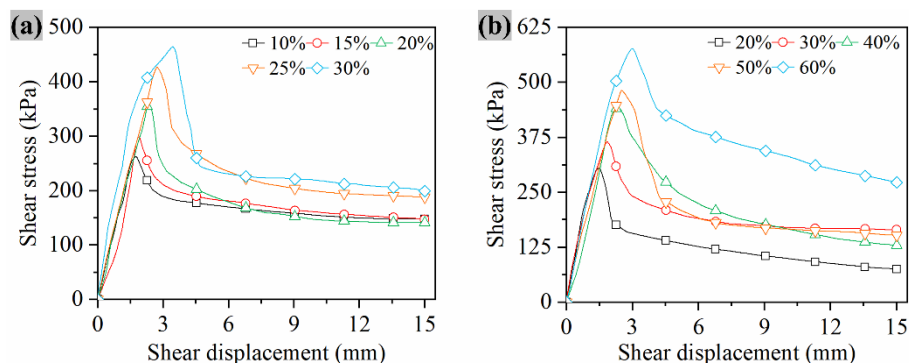
Figure 7. Shear stress–displacement curves for different debris contents (normal stress of 200 kPa, temperature of -20 ℃). **(a)** Shear stress–displacement curve of fine debris ice and **(b)** Shear stress-displacement curve of coarse debris ice.

225 **3.2.3 Shear stress-displacement curves for different ice types**

Polycrystalline ice, ice–rock composite, fine debris ice (30% debris content), and coarse debris ice (30% debris content) at the same temperature (-20 ℃) are shown in Fig. 8. In terms of peak strength, the samples are in the following order: fine debris ice (466 kPa) > coarse debris ice (367 kPa) > polycrystalline ice (259 kPa) > ice–rock composite (192 kPa). The ice–rock interface is a relatively weak area of glacial strength. For the same debris content, fine debris ice > coarse debris ice

230 (Section 3.2.2). Fine debris particles are smaller, more evenly distributed, have a larger specific surface area, and are easier to contact during shearing compared to coarse debris particles.
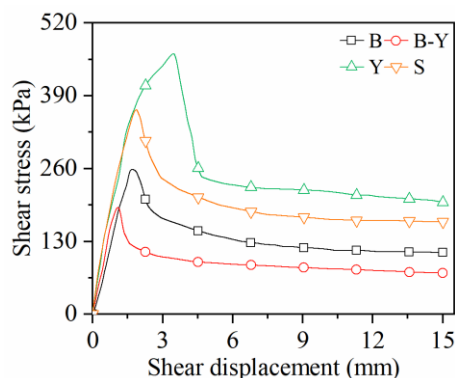
Figure 8. Shear stress-displacement curves for different ice types (normal stress of 200 kPa).

3.3 Shear strength of mountain glacier ice

235 The peak shear stress in the shear displacement-shear stress curve represents the shear strength. The slope and intercept of the normal stress-shear strength curve are the shear strength parameters in the Mohr-Coulomb failure criterion.

3.3.1 Shear strength at different temperatures

The shear strengths of polycrystalline ice at -0.5 °C under field and laboratory conditions are shown in Table 4. The shear strength of polycrystalline ice ranged be-tween 153 and 174 kPa in the field, while the shear strength of polycrystalline ice

240 ranged between 152 and 170 kPa in the laboratory and varied with the normal stress. The shear strength error between the field and laboratory polycrystalline ice was mainly within 5%, which met the requirements. The error increases as the normal stress increases, especially at 500 kPa, where the error is 5.2%. The analysis indicates that an increase in normal stress necessitates a longer pressurization time, resulting in a slight melting phenomenon in the absence of cooling measures during testing. Consequent-ly, the error rises with higher normal stress.

245 **Table 4.** Comparison of the shear strengths of field and laboratory polycrystalline ice

Temperature (°C)	Normal stress (kPa)	Shear strength (kPa)		Error (%)
		Gongga Glacier ice	Laboratory polycrystalline ice	
	100	153	152	-0.7
	200	169	170	0.6
-0.5	300	167	164	-1.8
	400	174	168	-3.4
	500	154	162	5.2

The shear strength and parameter curves of polycrystalline ice and ice–rock composites are shown in Fig. 9. The figure shows that the shear strengths of polycrystalline ice and ice–rock composites decrease with increasing temperature.

Polycrystalline ice shear strength decays nonlinearly with increasing temperature. The ice–rock composite shear strength

250   decays linearly with increasing temperature. At temperatures near 0 °C, normal stress has less impact on shear strength

compared to other temperatures (Figs. 9a and 9b). The internal friction angle of polycrystalline ice ranges from 1 to 26°

between -0.5 and -40 °C; the cohesion ranges from 155 to 187 kPa (Fig. 9c). The internal friction angle and cohesion

decrease nonlinearly with increasing temperature. The ice–rock composite direct tests resulted in an internal friction angle of

7–29° and cohesion of 110–172 kPa (Fig. 9d). With increasing temperature, both the internal friction angle and cohesion

255   decrease linearly. In summary, the shear strength and parameters of polycrystalline ice decrease nonlinearly with increasing

temperature, while the shear strength and parameters of the ice–rock composite decrease linearly. Even if the normal stress

increases, the shear strength will not change significantly at temperatures close to 0 °C.
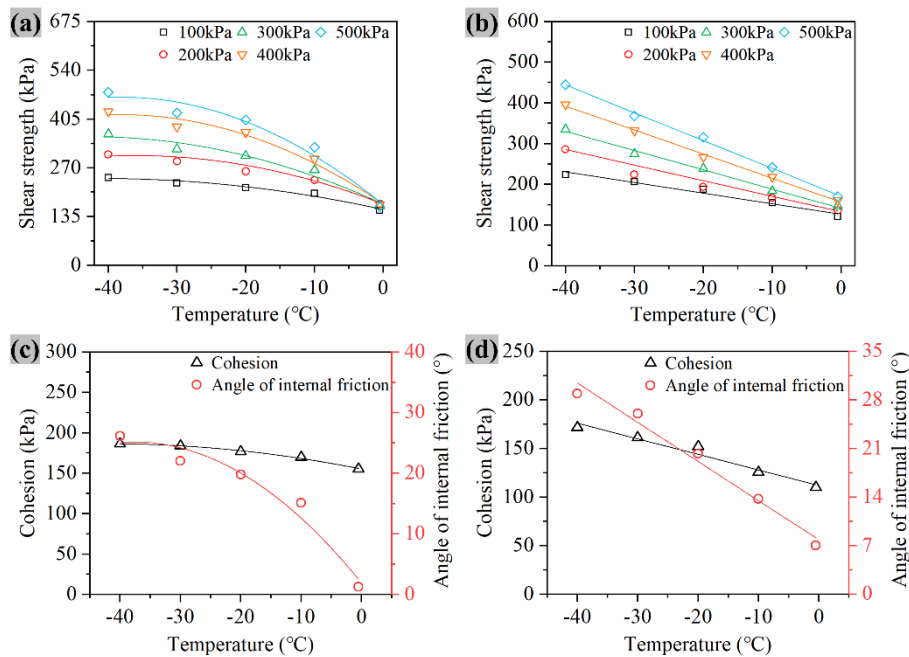
Figure 9. Shear strength characteristics of polycrystalline ice and ice–rock composites at different temperatures. **(a)** Shear strength-
260   temperature curve of polycrystalline ice. **(b)** Shear strength-temperature curve of ice–rock composite. **(c)** Shear strength parameters of polycrystalline ice. **(d)** Shear strength parameters of the ice–rock composite.

3.3.2 Shear strength at different debris contents

The shear strength and strength parameter curves of fine debris ice and coarse debris ice at -20 °C are shown in Fig. 10. The

shear strength of both fine debris ice and coarse debris ice exhibit nonlinear growth characteristics as the debris content

265   increases. In fine debris ice with 0-30% debris content, the internal friction angle ranges from 19 to 55 °, and the cohesion

ranges from 148 to 189 kPa. As the debris content increases, the internal friction angle and cohesion increase nonlinearly. In

coarse debris ice with 0–60% debris content, the internal friction angle ranges from 19 to 55°, and the cohesion ranges from

176 to 299 kPa. When the content increases beyond a certain value, the internal friction angles of both are higher than 45°.

The reason is that the debris particles increase, and the contact between particles is enhanced, similar to a soil-rock mixture's

270   shear and dilatation effect. In summary, the shear strength of debris ice increases nonlinearly with debris content. Its internal

friction angle first increases rapidly with debris content and then slows, while its cohesion initially increases slowly with

debris content and then rapidly increases.
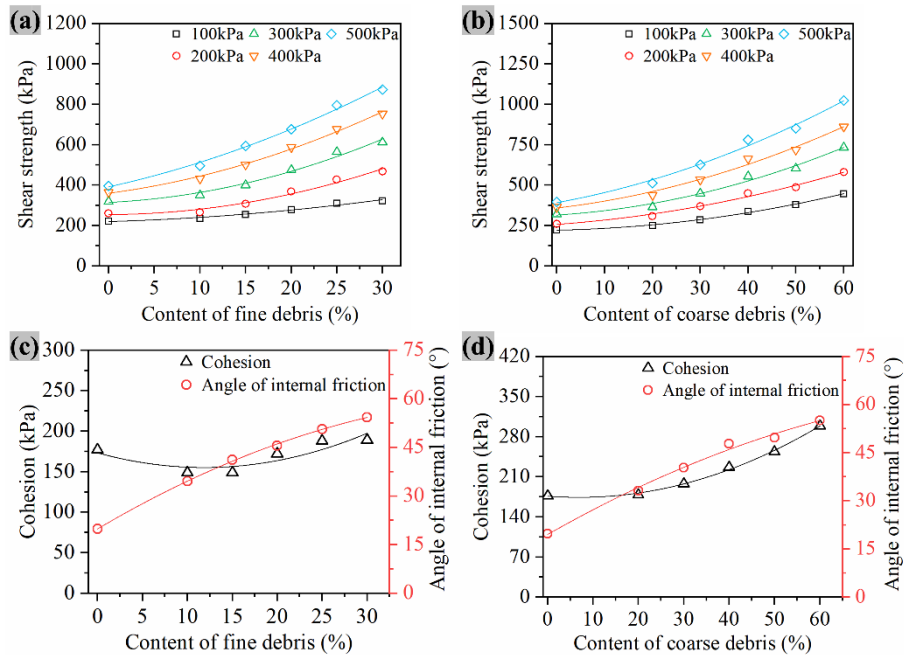
Figure 10. Shear strength characteristics of fine debris ice and coarse debris ice at different debris contents. **(a)** Shear strength–content
275   curve of fine debris ice. **(b)** Shear strength–content curve of coarse debris ice. **(c)** Shear strength parameters of fine debris ice. **(d)** Shear
strength parameters of coarse debris ice.

3.3.3 Shear strengths of different ice type

Due to the different designs of the content of fine debris ice and coarse debris ice, the two cannot be compared directly.

However, they can be compared through data fitting when the content is less than 30%. The fitting line of polycrystalline ice,

280   ice-rock composite at different temperatures, fine debris ice, and coarse debris ice under different debris contents is shown in

Fig. 11. At -20 °C, the relationship of shear strength among the four is fine debris ice > coarse debris ice > polycrystalline

ice > ice-rock composite (Section 3.2.3). At the same temperature and debris content, coarse debris ice has lower shear

strength than fine debris ice. This suggests that the specific surface area of fine debris ice is larger than that of coarse debris

ice, and the particle effect is stronger. Additionally, the shear strength of the ice-rock composite exceeds that of

285   polycrystalline ice at the same temperature and 0% debris content (Section 3.3.1).
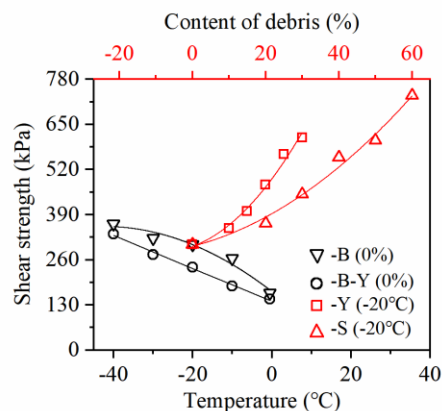
Figure 11. Shear strength characteristics of different ice types.

4 Discussion

Research indicates that the shear strength of polycrystalline ice displays nonlinear degradation as the temperature increases,
290 while the shear strength of ice-rock composites shows linear degradation with increasing temperature. Therefore, temperature has a more pronounced impact on the strength of polycrystalline ice. Debris ice display exhibits the strength of the nonlinear enhancements with increasing debris content. Additionally, the shear strength of fine and coarse debris ice exhibits nonlinear enhancements as the debris content increases. Fine debris ice exhibits the highest strength, followed by coarse debris ice, polycrystalline ice, and ice–rock composites. The ice–rock interface is a relatively weak area of glacial.
295 The ranking of strength between clean ice and debris ice as determined by our experiments (debris ice > clean ice, Huang et al.(2023a) results are also the same) does not align with the findings of Fitzsimons et al. (2024) (clean ice > laminated ice > massive ice). This difference is due to the uneven distribution of debris in the field ice, and the inhomogeneity leads to the failure to form a skeleton effect in the shear (Qi et al., 2018; Pei et al., 2022), a small number of particles will lead to a slight downward trend in cohesion (Fig.10c), which is also the reason why we did not carry out the shear test of debris ice
300 sampling in Gongga Glacier, and we failed to find a fairly uniform debris ice sampling site. Cao et al. (2022) found that clean ice has higher shear strength than the interface between ice and concrete, supporting our conclusion. The laminated ice shown in Fig. 7 in the study of Fitzsimons et al. (2024) corresponds to the failure surface (band) in the subglacial rock. The ice-rich debris–rock interface in the study of Huang et al. (2023b) is one of the failure surfaces (band) in Section 1. Due to the different experimental settings, we cannot give a complete ranking of glacial medium strength

305 **4.1 Inference of the strength degradation mechanism with increasing temperature**

As the temperature increases, the strength of polycrystalline ice declines, as reflected in previous studies (Shan et al., 2018). Furthermore, the shear strength of polycrystalline ice decays nonlinearly with temperature. This is inconsistent with linear or nearly linear relationships (Han et al., 2018) and the perspective that it first decreases and then increases (Zhang et al., 2022).

Different perspectives may arise due to experimental designs omitting temperature values close to the ice point, obscuring nonlinear relationships, or perhaps preferring near-linear relationships for computational ease. The difference between our studies and Zhang et al. (2022) is that they used single-crystal and brine ice. This relationship is inextricably linked to polycrystalline ice characteristics. Fish and Zaretsky, (1997) consider ice at -10 °C an ideal cohesive material with an internal friction angle of 0. In polycrystalline ice, recrystallization is more likely when the temperature exceeds -10 °C (Cuffey and Paterson, 2010; Ren et al., 2020). Analysis suggests that the recrystallization of polycrystalline ice under the influence of temperature produces this nonlinear relationship. Fitzsimons et al. (2024) found that glacier basal ice at -18 °C had a shear strength of 1.21 MPa, which differs significantly from our laboratory's data for clean ice at -20 °C (0.26 MPa shear strength). This difference is mainly due to the formation conditions of on-site and indoor samples. The clean ice of real glaciers takes tens of thousands of years to form, while our clean polycrystalline ice samples are formed by the rapid compression and freezing of broken ice, so there is a gap in strength with the field. This does not impact our analysis of how shear strength changes with temperature (trend analysis), as we have also tested clean ice strength near 0 °C in the field. The strength of clean ice near the freezing point is certainly low (Huang et al. (2023a)).

It is a common view that the increase in temperature leads to the degradation of the strength of the ice–solid composite. Specifically, this characteristic is demonstrated in ice-rock composite shear tests. Furthermore, the shear strength of the ice–rock composite linearly decays with increasing temperature. This finding is similar to McCarthy et al. (2017), Work and Lian, (2018), and Cao et al. (2022), who have similar conclusions on rock joint–ice and ice–concrete structures. Cao et al. (2022) showed that the shear strength decreased by about 10% when the temperature ranged from -8 °C to -4 °C. Our shear strength is reduced more significantly (-10 °C to -0.5 °C, 20-23% reduction in shear strength, related to normal stress), and this difference is due to the properties of the interfacial materials. According to Su et al. (2024), under conditions of constant normal stress and roughness, a decrease in temperature from -10 °C to -50 °C results in an increase of 0.3 MPa in shear strength. The variation in strength with temperature that we measured is consistent with his findings, showing an increase of about 0.2 MPa from -10 °C to -40 °C. For other situations of failure surface (band), it can also be effectively supplemented. Huang et al. (2023b) studied the shear strength of the ice-rich debris–rock interface and found that the shear strength parameter decreased linearly with the increase in temperature. When the temperature increased from -9 °C to -1 °C, the shear strength decreased by about 78%. Meng et al. (2024) and Su et al. (2024) studied the interfacial strength of ice-rich debris–rock interface and ice-rock interfacial strength under the interfacial fluctuation respectively.

4.1.1 Mechanism of polycrystalline ice strength degradation

To describe the strength degradation process of polycrystalline ice under the influence of temperature, we try to generalize this process. Specifically, the shearing process can be divided into four phases (Fig. 12c). **(I)** The grain boundary is the most prominent planar defect. Under shear stress, cracks begin to nucleate at some grain boundaries (Chen et al., 2020). A bubble of air in polycrystalline ice causes the grains to soften (Gagnon and Gammon, 1995), and under shear squeezing, air migrates along grain boundaries. **(II)** As shear stress increases, there is an increase in tensile stress in the crystal axis direction. Cracks

continue to expand and merge, and some air is released. The crystal-preferred orientation of small grains is relatively weak at low temperatures (Liebl, 2021). Grain boundary mobility decreases (Fan, 2021), and shear bands sprout and expand irregularly. At high temperatures, dynamic recrystallization on the grain scale leads to the reorganization of bubbles and
345 grain boundaries (Journaux et al., 2019) and polycrystalline ice volume shrinkage. Grain boundaries tend to migrate to form lobed grain boundaries (Qi et al., 2019; Liebl, 2021). Grains exhibit irregular shapes, strain-induced grain boundary migration (GBM) toward easy slip, and shear zone budding and expansion. **(III)** As shear displacement increases, cracks extend and merge, and shear zones are penetrated. Polycrystalline ice splits in crack extension at low temperatures, showing that splitting precedes fragmentation. At high temperatures, dynamic recrystallization of polycrystalline ice leads to ice
350 softening (Wilson et al., 2020) or melting to form aqueous films (Mizukami and Maeno, 2000), resulting in a decrease in shear interfacial resistance and allowing the shear zone to penetrate. **(IV)** A shear surface is formed after shear failure. At low temperatures, the shear fracture is rough, and clear shear marks appear (Figs. 12a and 12c). At high temperatures, the shear fracture is smooth, and liquid water appears on the shear surface (Figs. 12b and 12c).
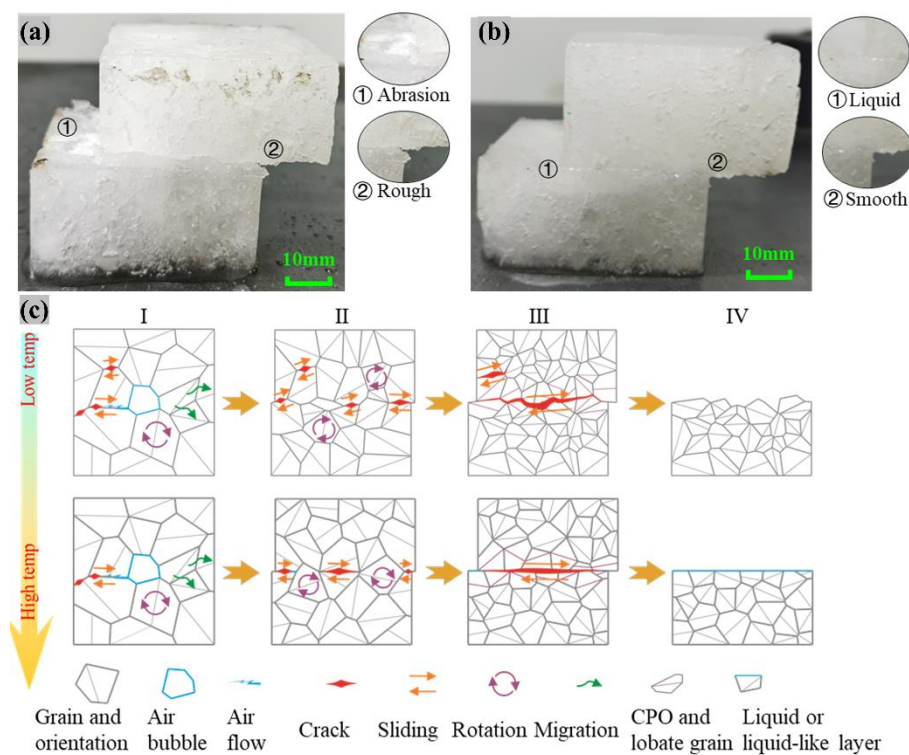
355 **Figure 12.** Failure mechanism of polycrystalline ice. **(a)** Post-failure samples of polycrystalline ice (low temperature). **(b)** Post-failure samples of polycrystalline ice (high temperature). **(c)** Shear failure evolution processes of polycrystalline ice (according to Fan, (2021) and Qi et al. (2019) modification).

4.1.2 Mechanism of ice–rock composite strength degradation

Similarly, to describe the strength degradation process in ice-rock composites influenced by temperature, we attempt to
360 generalize this process. Specifically, the shearing process can be divided into four phases (Fig. 13 c). **(I)** In the case of weak
ice–rock interfaces, tensile stress is generated, leading to cracks (Westerveld, 2020). Air bubbles migrate and compress
within polycrystalline ice. **(II)** As the stress concentrates on sharp parts of the interface and defects, the ice filling the micro
defects is melted or sheared, and the anchor effect is weakened (Aoyama et al., 2006). Polycrystalline ice undergoes pressure
melting (Emelyanenko et al., 2020; Boinovich et al., 2022; Wang et al., 2023). At low temperatures, recrystallization occurs
365 (Ren et al., 2020), resulting in a change in crystal axis orientation, and some ice crystals break into fragments: this breakage
interface wear, irregular shear bands, and increased friction at the interface. The polycrystalline ice melts rapidly at high
temperatures, and the interfacial cracks expand horizontally from the ends as liquid water migrates (Bashiru et al., 2006).
(III) At low temperatures, the interfacial friction increases as the shear displacement increases, and the interfacial crack
extends in a brittle manner. High temperatures increase the presence of liquid water at the ice–rock interface, lubricating and
370 filling defects and extending interfacial cracks (Adams et al., 2021). **(IV)** A shear surface is formed after shear failure (Figs.
13a and 13b). There are nondominant cracks, ice crumbs that fall off to fill defects, and interfacial wear scratches after low-
temperature shearing (Figs. 13a and 13c). At high temperatures, the shear fracture is relatively flat, liquid water can be seen
at the interface, and there are signs of wetting on the rock block (Figs. 13b and 13c).
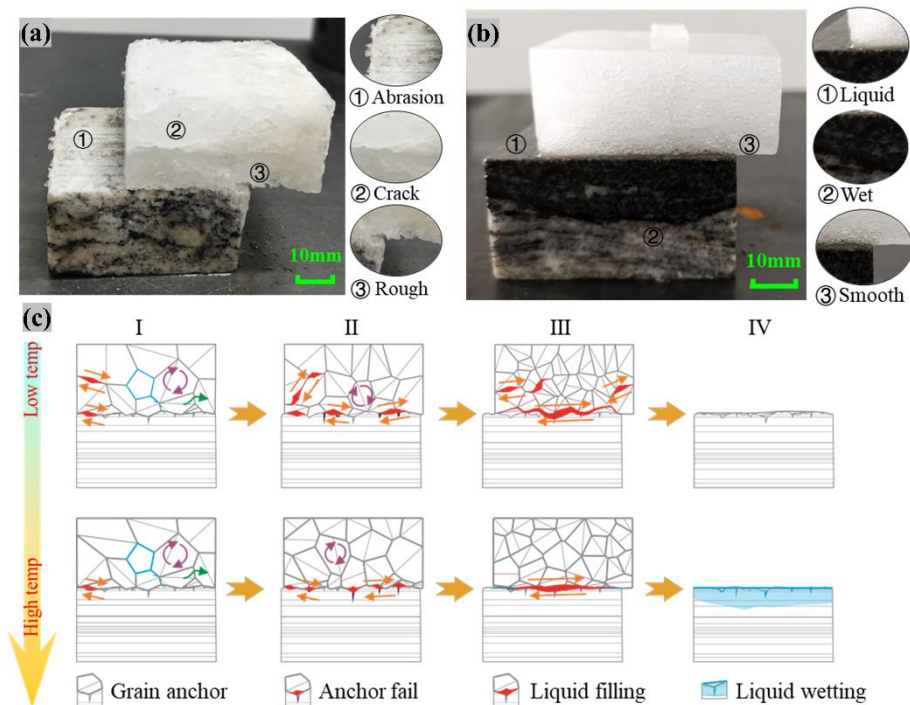
Figure 13. The failure mechanism of ice–rock composites. **(a)** Postfailure samples of ice–rock composites (low temperature). **(b)** Postfailure samples of ice–rock composites (high temperature). **(c)** Shear failure evolution processes of ice–rock composites (according to Fan, (2021), Qi et al. (2019), and Aoyama et al. (2006) modification).

4.2 Inference of strength reinforcement mechanism with increased debris content

The increase in debris content enhances the strength of glacier ice, as reflected in Lijith et al. (2022) and Huang et al. (2023a), who have similar conclusions on frozen sand, frozen soil, and moraine soil. They have a nonlinear relationship, consistent with Goughnour and Andersland, (1968), although they tend to describe them with piecewise functions. Moreover, the concentration of debris enhances strength because the specific surface area of the debris increases, resulting in a larger contact area with the ice crystals. When the ice content of the frozen debris increases from 0% (undersaturation) to 25% (saturation), the shear strength of the sample increases significantly, which is reflected as a nonlinear increase in our study. In contrast, the shear strength of the sample decreases as the ice content continues to increase (Nickling and Bennett (1984)). Although we do not have the broad debris content of Nickling and Bennett (1984), our study found that the strength of fine debris ice is higher than that of coarse debris ice. Moore (2014) conducted a normalization of strength and creep stress test data for debris-ice mixtures, which included clean ice with a clastic volume fraction of 0. The findings indicated that fine particles had a higher capacity to retain unfrozen water compared to coarse particles at temperatures below the freezing point. That doesn't seem to fit with the conclusions we've drawn, but it doesn't. Although fine debris ice is more likely to support liquid water, this liquid water does not directly lead to increased shear strength. More importantly, the larger contact area, the more significant capillary action, and the tighter structure of the fine debris ice combine to give them greater shear strength than coarse debris ice. It can be seen from Fig. 8 that to reach the peak shear stress, a larger displacement will be moved to promote the contact of fine particles. In addition, to highlight the influence of temperature on the shear strength of ice-rich debris, Fu et al. (2021) and Huang et al. (2023a) studied the influence of ice melting on the mechanical properties of debris ice, which expanded our research and made the study of the main failure surface (band) of ice avalanche (including ice-rock avalanche) more systematic.

Similarly, we generalize this process to describe the strength degradation process of debris ice under the influence of debris content. The shearing process can be divided into four phases (Fig. 14c). **(I)** Cracks initiate in stress concentration areas, and the air is migrated or exhausted through the cracks. Air bubbles decrease, causing a reduction in volume (Arenson and Springman, 2005). **(II)** In debris ice, particles are displaced (rotated or moved), some are in direct contact, and bonds between particles and ice crystals break (Li et al., 2022a). There is an increased density of dislocations (Middleton et al., 2017). Gravel contact with high debris content gradually transitions to partial surface contact, enhancing the skeleton effect of glacial ice, and subsequent stages are dominated by particle squeezing and sliding (Qi et al., 2018; Pei et al., 2022). **(III)** Cracks continue to expand, and due to the pinning effect (Durham et al., 1992; Moore, 2014), cracks bypass particles and gradually form a dominant shear plane. A high debris-content ice crystal can break into fragments (especially between and around particles), shear squeezing causes a new equilibrium network structure between fragments, and particle squeezing and breakage cause shear zone volume expansion (Li and Aydin, 2010; Lijith et al., 2022). **(IV)** A shear surface is formed

after shear failure. After unloading, some particles fall off (Li et al., 2022b). Cracks bypassing debris can be seen on the
410   fracture surface of debris ice (Fig. 14a). The shear surface of the coarse debris ice can show a large amount of debris
squeezed together, showing a lodging shape accompanied by particle breakage. There are cracks at the junction of
polycrystalline ice and debris (Fig. 14b).
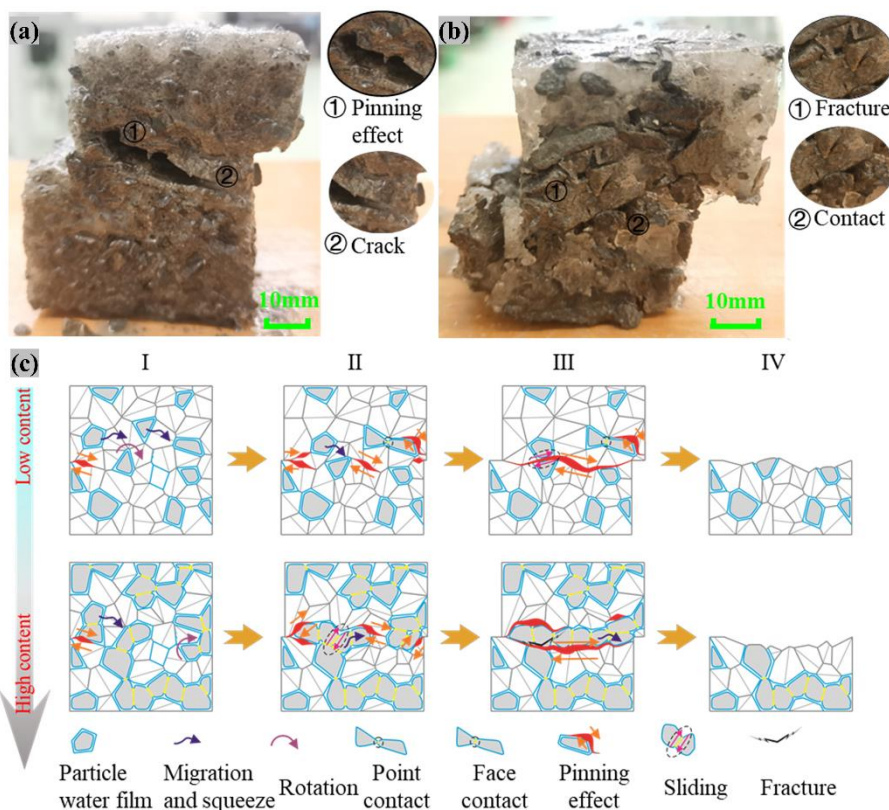
Figure 14. Failure mechanism of debris ice. **(a)** Postfailure samples of fine debris ice (high content). **(b)** Postfailure samples of coarse
415   debris ice (high content). **(c)** Shear failure evolution processes of debris ice (according to Fan (2021), Qi et al. (2019), and Ting et al. (1983)
modification).

4.3 Future work: Application of failure mechanism and data

The main components of IA are ice and debris. The material of the landslide is rock and soil. Both IA and landslide are
large-scale macroscopic phenomena of material failure. Both of them are the release behavior of slope materials to the free
420   face (Fig. 15), which will form a shear zone (also referred to as strain localization) or slip zone due to shear localization (Xu
et al., 2004), which promoted its softening behavior at the sample scale (Section 3.2; Section 4.1; Section 4.2; Zhang, 2004),
and showed the gradual expansion of shear zone or slip zone (Fig. 15, red zone) at the disaster scale (Dai and Lu, 2006; Tan
et al., 2016; Lu et al., 2017) until an IA occurred in the sliding zone penetration. As global warming intensifies, mountain
glacial ice temperatures continue to increase. The glacier stress begins to adjust, and the strain localization occurs
425   (Fitzsimons et al., 2024) when the stress level rate reaches the shear strength of the material (Section 3.3) at the stress

concentration site (Fig. 15). Glacial stability trends, such as providing base slip friction parameters (Section 3.3) in glacier dynamics simulations (Li et al., 2023), can be predicted by understanding how strength weakens under increased temperatures. Farinotti et al. (2019) shared key fundamental data (global glacier thickness data), while thermodynamic methods can be used to retrieve glacier base temperature, our study data and existing results data (e.g. Nickling and Bennett

430 (1984); Fish and Zaretsky, (1997); Fu et al. (2021); Huang's team (Huang et al. (2023a); Huang et al. (2024b); Meng et al. (2024)); Su et al. (2024); And so on) complement each other, making it statistically significant. The formula or interpolation fitted with these data can determine the shear strength of the failure surface of the glacier at the calculated basement temperature, and the ratio of the shear strength of the failure surface to the driving force of the basement can be used as an important reference index to evaluate the stability of the glacier (Fig. 15), which is reflected in Fig. 9 in the research of

435 Gilbert et al., (2018). Wei et al., (2024) more clearly reflects the value of such research results. More convenient and simple applications are better reflected in their research (Smith, 2004; Nater et al., 2008; Loche, 2023; Fiolleau et al.,2024). Future focus should be placed on the issue of deformation evolution near the melting point of glacial ice, and the theoretical construction of the near-melting point system of glaciers should be advanced. As glaciers continuously erode and transport rock bodies, they may mix with additional debris, resulting in a darker color. To understand rock glaciers' future energy

440 accumulation and stability trend, researchers must investigate the strength enhancement that occurs with increased debris content. Other scholars are also studying the deformation evolution issue of rock glaciers.
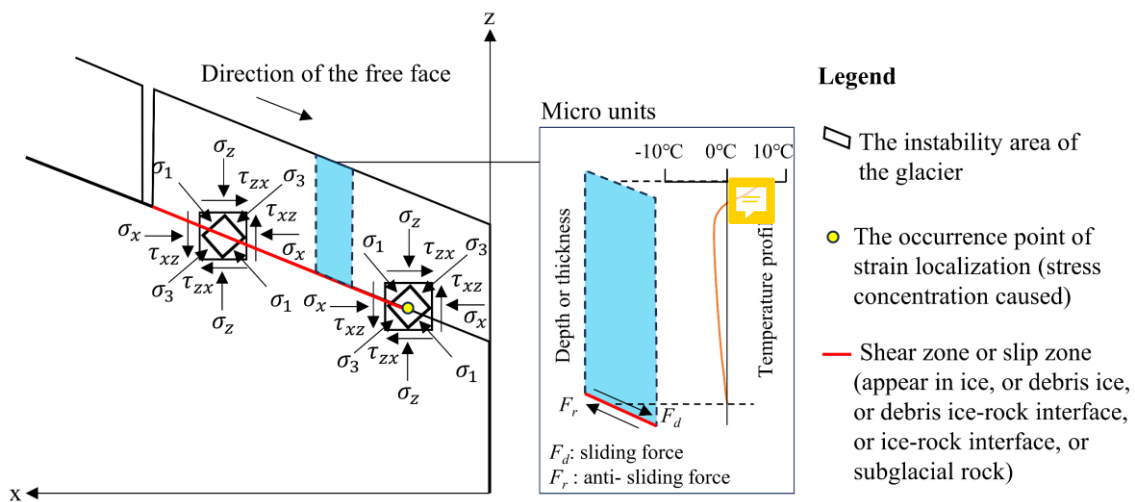
Figure 15. IA formation mechanism (τ is the shear stress, σ_x is the stress of x direction, σ_z is the stress of z direction (self-weight stress), σ_1 is the maximum principal stress, σ_3 is the minimum principal stress), $\boldsymbol{F_d}$ is the sliding force, $\boldsymbol{F_r}$ is the anti-sliding force (the shear strength is included in this term).

5 Conclusion

Previous research on ice mechanics has predominantly centered on sea, river, atmospheric, and permafrost ice, leaving the shear strength characteristics of mountain glacier ice less understood. To address this gap, we selected the Gongga Mountain glacier as our main study site, aiming to comprehensively investigate the shear strength characteristics of glacier ice under varying temperatures and debris contents. In situ studies at the Gongga Glacier examined glacial ice properties, with direct shear tests conducted at -0.5 °C under normal stresses ranging from 100 to 500 kPa. These tests established a baseline for indoor reshaped polycrystalline ice's physical and mechanical properties. Further tests on polycrystalline ice and ice–rock composites were performed at temperatures of -0.5, -10, -20, -30, and -40 °C, using remodeled polycrystalline ice, gneiss under the same range of normal stresses. Direct shear tests were carried out on fine and coarse debris ice with fine debris contents of 10, 15, 20, 25, and 30% and coarse debris contents of 20, 30, 40, 50, and 60% under identical normal stresses. The variations in deformation failure and shear strength for glacier ice under different conditions were obtained, and the deformation evolution process and shear strength mechanism were analyzed. The four main conclusions were as follows:

(1) Debris content positively correlates with density, and the porosity exhibits a nonlinear decreasing trend.

(2) There is strain softening in the shearing process. The peak strength is displayed for different types of ice: fine debris ice (466 kPa) > coarse debris ice (367 kPa) > polycrystalline ice (259 kPa) > ice–rock composite (192 kPa).

(3) Polycrystalline ice displays the strength of nonlinear degradation with increasing temperature and ice–rock composites show the strength of linear degradation with increasing temperature display strength degradation with increasing temperature. Fine and coarse debris ice display exhibits the strength of the nonlinear enhancements with increasing debris content.

(4) We discussed the mechanism by which the strength of polycrystalline ice and ice–rock composites degrade with increasing temperature. We believe that the emergence of liquid water is one of the reasons for the degradation of strength, which can be clearly observed in the destructive samples; also, the mechanism by which the increase in debris content leads to the strength enhancement of debris ice is discussed. It is believed that solid particle effects (biting, friction, and crushing) are essential reasons for strength enhancement, which can also be observed in destructive samples.

These results emphasize the importance of considering both debris content and temperature changes in the development of models for predicting the behavior of ice masses under stress. Data can be used in glacier dynamics simulation parameters, which is crucial for designing and implementing effective avalanche mitigation and disaster prevention strategies. Understanding these variables is essential for strategically developing mitigation measures and disaster prevention practices, ultimately contributing to the safety and sustainability of mountainous regions prone to ice avalanches.

Author contributions

Minggao Tang: Conceptualization, Data curation, Funding acquisition, Validation, Supervision, Resources, Writing – review & editing. **Huanle Zhao:** Formal Analysis, Investigation, Methodology, Validation, Writing – original draft, Writing

– review & editing. **Qiang Xu:** Funding acquisition, Project administration. **Wentao Ni:** Formal Analysis, Investigation, Resources, Validation, Writing – original draft. **Guang Li:** Writing – original draft, Visualization. **Zhiping Zuo:** Investigation, Visualization. **Xu Chen:** Methodology, Writing – review & editing. **Yihua Zhong:** Writing – review & editing.

Competing interests

The authors declare that they have no known competing financial interests or personal relationships that could have appeared to influence the work reported in this paper.

Financial support

This research was supported by the Second Tibetan Plateau Scientific Expedition and Research Program (STEP) (Grant No. 2019QZKK0201), the National Natural Science Foundation of China (Grant No. 42377199, 41941019), Chengdu University of Technology Postgraduate Innovative Cultivation Program (Grant No. CDUT2023BJCX008), State Key Laboratory of Geohazard Prevention and Geoenvironment Protection Independent Research Project (Grant No. SKLGP2021Z005).

References

Adams, C. J. C., Iverson, N. R., Helanow, C., Zoet, L. K., and Bate, C. E.: Softening of temperate ice by interstitial water, Frontiers in Earth Science, 9, 702761, https://doi.org/10.3389/feart.2021.702761, 2021.

Aoyama, T., Ishikawa, M., Hira, T., and Ukigai, K.: Effect of surface rough-ness on adhesive shear strength between pure ice and a solid surface, Proceedings of the Japan Refrigeration and Air Conditioning Society, 23, 273-281, https://doi.org/10.11322/tjsrae.23.273, 2006 (in Japanese).

Arenson, L. U., and Springman, S. M.: Mathematical descriptions for the behaviour of ice-rich frozen soils at temperatures close to 0 °C, Canadian Geotechnical Journal, 42, 431-442, https://doi.org/10.1139/t04-109, 2005.

Bashiru, A., Zhang, Y. B., Zhang, H. Q.: Numerical simulation of ice–rock interface under shear loading, in: ISRM International Symposium 2006: 4th Asian Rock Mechanics Symposium, Singapore, 8-10 November 2006, 458, 2006.

Boinovich, L. B., Emelyanenko, K. A., and Emelyanenko, A. M.: Superhydrophobic versus SLIPS: Temperature dependence and the stability of ice adhesion strength, Journal of Colloid and Interface Science, 606, 556-566, https://doi.org/10.1016/j.jcis.2021.08.030, 2022.

Bondesan. A. and Francese, R. G.: The climate-driven disaster of the Marmolada Glacier (Italy), Geomorphology, 431, 108687, https://doi.org/10.1016/j.geomorph.2023.108687, 2023.

Cao, X. L., Mo, H. M., Zhang, G. L., Zhang, Q. W., and Fan, F.: Experimental study on shear strengths of ice-roof interface

505   aiming the study of roof snow sliding, Frontiers in Earth Science, 10, 862134, https://doi.org/10.3389/feart.2022.862134, 2022.

Cuffey, K. M., and Paterson, W. S. B.: The physics of glaciers. Academic Press, America, ISBN 978-0-12-369461-4, 2010.

Chen, G., Kong, W. L., and Wang, F. X.: Experimental study on ice shear strength evolution, in: Proceedings of the International Conference on Aerospace System Science and Engineering, Shanghai, 14–16 July 2020, 71-89, 2020.

510   Dai, Z. H., and Lu, C. J.: Mechanical explanations on mechanism of slope stability, Chinese Journal of Geotechnical Engineering, 28, 1191-1197, 2006, (in Chinese).

Dubey, S., Sattar, A., Goyal, M. K., Allen, S., Frey, H., Haritashya, U. K., and Huggel, C.: Mass movement hazard and exposure in the Himalaya, Earth's Future, 11, e2022EF003253, https://doi.org/10.1029/2022EF003253, 2023.

Durham, W. B., Kirby, S. H., and Stern, L. A.: Effects of dispersed particulates on the rheology of water ice at planetary

515   conditions, Journal of Geophysical Research: Planets, 97, 20883-20897, https://doi.org/10.1029/92JE02326, 1992.

Emelyanenko, K. A., Emelyanenko, A. M., and Boinovich, L. B.: Water and ice adhe-sion to solid surfaces: Common and specific, the impact of temperature and surface wettability, Coatings, 10, 648, https://doi.org/10.3390/coatings10070648, 2020.

Farinotti, D., Huss, M., Fürst, J. J., Landmann, J., Machguth, H., Maussion, F., and Pandit, A.: A consensus estimate for the

520   ice thickness distribution of all glaciers on Earth, Nature Geoscience, 12, 168-173, https://doi.org/10.1038/s41561-019-0300-3, 2019.

Fan, S.: The evolution of deformation mechanisms during the mechanical weakening of polycrystalline ice: a quantitative microstructural study, PhD thesis, University of Otago, Dunedin, New Zealand, 440 pp, 2021.

Farid, H., Saeidi, A., and Farzaneh, M.: Prediction of failure in atmospheric ice under triaxial compressive stress, Cold

525   Regions Science and Technology, 138, 46-56, https://doi.org/10.1016/j.coldregions.2017.03.005, 2007.

Fish, A. M., and Zaretsky, Y. K.: Ice strength as a function of hydrostatic pressure and temperature, CRREL report, http://purl.access.gpo.gov/GPO/LPS13422. 3820781, 22pp., 1997.

Fiolleau, S., Uhlemann, S., Shirley, I., Wang, C., Wielandt, S., Rowland, J., and Dafflon, B.: Insights on seasonal solifluction processes in warm permafrost Arctic landscape using a dense monitoring approach across adjacent hillslopes, Environmental

530   Research Letters, 19, 044021, https://doi.org/10.1088/1748-9326/ad28dc, 2024.

Fitzsimons, S., Samyn, D., and Lorrain, R.: Deformation, strength and tectonic evolution of basal ice in Taylor Glacier, Antarctica, Journal of Geophysical Research: Earth Surface, 129, e2023JF007456, https://doi.org/10.1029/2023JF007456, 2024.

Fu, Y. J., Jiang, Y., Wang, J., Liu, Z. M., and Lu, X. S.: Mechanical properties of frozen glacial tills due to short periods of

535   thawing, Frontiers in Earth Science, 9, 799467, https://doi.org/10.3389/feart.2021.799467, 2021.

Gagnon, R. E., and Gammon, P. H.: Characterization and flexural strength of iceberg and glacier ice, Journal of Glaciology, 41, 103-111, https://doi.org/10.3189/S0022143000017809, 1995.

Goughnour, R. R., and Andersland, O. B.: Mechanical properties of a sand-ice system, Journal of the Soil Mechanics and Foundations Division, 94, 923-950, https://doi.org/10.1061/JSFEAQ.000117, 1968.

540 Gilbert, A., Leinss, S., Kargel, J., Kääb, A., Gascoin, S., Leonard, G., Berthier, E., Karki, A., and Yao, T. D.: Mechanisms leading to the 2016 giant twin glacier collapses, Aru Range, Tibet, The Cryosphere, 12, 2883-2900, https://doi.org/10.5194/tc-12-2883-2018, 2018.

Guo, Y. K., and Meng, W. Y.: Experimental investigations on mechanical properties of ice, Journal of North China University of Water Resources and Electric Power (Natural Science Edition), 36, 40-43, https://doi.org/10.3969/j.issn.1002-

545 5634. 2015.03.010, 2015 (in Chinese).

Han, H. W., Xie, F., Wang, E. L., and Zhang, D.: Experimental study on properties of compressive strength and failure criteria of river ice under triaxial compression, Shuili Xuebao, 49, 1199-1206, https://doi.org/10.13243/j.cnki.slxb.20180148, 2018 (in Chinese).

Huang, D., Meng, Q. J., Song, Y. X., Gu, D. M., Peng, J. B., and Zhong, Z.: Experimental investigation on shear

550 performance degradation of ice-rich debris under thawing, Cold Regions Science and Technology, 212, 103889, https://doi.org/10.1016/j.coldregions.2023.103889, 2023a.

Huang, D, Meng, Q. J., Song, Y. X., Gu, D. M., Cen, D. F., and Zhong, Z.: Experimental study on the shear mechanical behavior of ice-rich debris–rock interface: effects of temperature, stress, and ice content, Canadian Geotechnical Journal, 61, 1051-1072, https://doi.org/10.1139/cgj-2023-0375, 2023b.

555 IPCC.: Sections. In Climate Change 2023: Synthesis Report. Contribution of Working Groups I, II and III to the Sixth Assessment Report of the Intergovernmental Panel on Climate Change [Core Writing Team, H. Lee and J. Romero (eds.)]. IPCC, Geneva, Switzerland, pp 35-115. https://doi.org/10.59327/IPCC/AR6-9789291691647, 2023.

Ji, S. Y., Liu, H. L., Li, P. F., and Su J.: Experimental studies on the Bohai sea ice shear strength, Journal of Cold Regions Engineering, 27, 244-254, https://doi.org/10.1061/(ASCE)CR.1943-5495.0000060, 2013.

560 Journaux, B., Chauve, T., Montagnat, M., Tommasi, A., Barou. F., Mainprice, D., and Gest, L.: Recrystallization processes, microstructure and crystallographic pre-ferred orientation evolution in polycrystalline ice during high-temperature simple shear, The Cryosphere, 13, 1495-1511, https://doi.org/10.5194/tc-13-1495-2019, 2019.

Kääb, A., Leinss, S., Gilbert, A., Bühler, Y., Gascoin, S., Evans, S. G., Bartelt, P., Bartelt, E., Brun, F., Chao, W. A., Farinotti, D., Gimbert, F., Guo, W. Q., Huggel, C., Kargel, J. S., Leonard, G. J., Tian, L. D., Treichler, D., and Yao, T. D.:

565 Massive collapse of two glaciers in western Tibet in 2016 after surge-like instability, Nature Geosci-ence, 11, 114-120, https://doi.org/10.1038/s41561-017-0039-7, 2018.

Kutliyarov, D., Ryzhkov, I., Kutliyarov, A., Khafizov, A., and Zubairov, R.: Role of accuracy and quantity of field tests in engineering-geotechnical researches for construction, Scientific Review Engineering and Environmental Sciences, 29, 421-434, https://doi.org/10.22630/PNIKS.2020.29.4.36, 2020.

570 Li, X., Yan, Y., and Ji, S. Y.: Mechanical properties of frozen ballast aggregates with different ice contents and temperatures, Construction and Building Materials, 317, 125893, https://doi.org/10.1016/j.conbuildmat.2021.125893, 2022a.

Li, X., Yan, Y., and Ji, S. Y.: Influence of ice content on strength and deformation characteristics of frozen ballast aggregate in cold region railway by experiments, Journal of railway science and engineering, 19, 697-705, https://doi.org/10.19713/j.cnki.43-1423/u.t20210286, 2022b (in Chinese).

575 Li, Y., Cui, Y. F., Hu, X., Lu, Z., Guo, J., Wang, Y., Wang, H., Wang, S. F., and Zhou, X. Z.: Glacier retreat in Eastern Himalaya drives catastrophic glacier hazard chain, Geophysical Research Letters, 51, e2024GL108202, https://doi.org/10.1029/2024GL108202, 2024.

Li, Y., Tang, M. G., Shuai, Y. Y., Zhao, H. L., Li, C. R., Ni, W. T., and Li, G.: Inversion and prediction simulation study of Aru Ice Avalanche-Debris flow motion pro-cess. Journal of Disaster Prevention and Mitigation Engineering [preprint],

580 http://kns.cnki.net/kcms/detail/32.1695.P.20231214.1834.002.html, 15 December 2023 (in Chinese).

Li, Y. R., and Aydin, A.: Behavior of rounded granular materials in direct shear: Mechanisms and quantification of fluctuations, Engineering Geology, 115, 96-104, https://doi.org/10.1016/j.enggeo.2010.06.008, 2010.

Liebl, C.: Microstructural evolution of ice under simple shear deformation. Dissertation, Master thesis, University of Gothenburg, Gothenburg, Sweden, 129 pp, 2021.

585 Lijith, K. P., Sharma, V., and Singh, D. N.: Shear strength characteristics of frozen fine sands under direct shear testing conditions, International Journal of Geomechanics, 22, 04021268, https://doi.org/10.1061/(ASCE)GM.1943-5622.0002228, 2022.

Loche, M.: Thermo-hydro-mechanical coupling in slope stability: advanced experiments and multiscale modelling, PhD thesis, Charles University, Prague, The Czech Republic, 111 pp, 2023.

590 Lu, Y. F., Huang, X. B., and Liu, D. F.: Distribution characteristics of force and stability analysis of slope, Chinese Journal of Geotechnical Engineering, 39, 1321-1329, https://doi.org/10.11779/CJGE201707019, 2017 (in Chinese).

McCarthy, C., Savage, H., and Nettles, M.: Temperature dependence of ice-on-rock friction at realistic glacier conditions, Philosophical Transactions of the Royal Society A: Mathematical, Physical and Engineering Sciences, 375, 20150348, https://doi.org/10.1098/rsta.2015.0348, 2017.

595 Meng, Q. J., Huang, D., Song, Y. X., Peng, J. B., Zhong, Zhu., and Huang, W. B.: Experimental study on the shear behavior of saw-toothed ice-rich debris–rock interface: effects of undulation, ice content, normal stress, and temperature, Bulletin of Engineering Geology and the Environment, 83, 1-23, https://doi.org/10.1007/s10064-024-03702-0, 2024.

Middleton, C. A., Grindrod, P. M., and Sammonds, P. R.: The effect of rock particles and D_2O replacement on the flow behaviour of ice, Philosophical Transactions of the Royal Society A: Mathematical, Physical and Engineering Sciences, 375,

600 20150349, https://doi.org/10.1098/rsta.2015.0349, 2017.

Ministry of Water Resources of the People's Republic of China.: GB/T 50123-2019 Geotechnical test method standard. China Planning Press, Beijing, China, 2019 (in Chinese).

Mizukami, N., and Maeno, N.: Normal stress dependence of ice-ice friction coefficients, Journal of the Japanese Society of Snow and Ice, 62, 515-521, https://doi.org/10.5331/seppyo.62.515, 2000 (in Japanese).

605   Moore, P. L.: Deformation of debris-ice mixtures, Reviews of Geophysics 52, 435-467, https://doi.org/10.1002/2014RG000453, 2014.

Nater, P., Arenson, L. U., Springman, S. M.: Choosing geotechnical parameters for slope stability assessments in alpine permafrost soils[C]//Ninth International Conference on Permafrost, University of Alaska Fairbanks. 29, 1261-1266, 2008.

Nickling, W. G., and Bennett, L.: The shear strength characteristics of frozen coarse granular debris, Journal of Glaciology, 610   30, 348-357, https://doi.org/10.3189/S0022143000006201, 1984.

Pei, Z., Liu, Y., and Luo, F.: Particle breakage behavior in frozen sands during triaxial shear tests based on the energy principle, Cold Regions Science and Technology, 199, 103571, https://doi.org/10.1016/j.coldregions.2022.103571, 2022.

Qi, C., Stern, L. A., Pathare, A., Durham, W. B., and Goldsby, D. L.: Inhibition of grain boundary sliding in fine-grained ice by intergranular particles: Implications for planetary ice masses, Geophysical Research Letters, 45, 12,757-12,765. 615   https://doi.org/10.1029/2018GL080228, 2018.

Qi, C., Prior, D. J., Craw, L., Fan, S., Llorens, M. G., Griera, A., Negrini, M., Bons, P. D., and Goldsby, D. L.: Crystallographic preferred orientations of ice deformed in direct-shear experiments at low temperatures, The Cryosphere, 13, 351-371, https://doi.org/10.5194/tc-13-351-2019, 2019.

Ren, J. W., Sheng, Y., Li, Z. Q., Che, T., and Li, C. J.: The Cryospheric Physics. Science Press, Beijing, China, pp 169., 620   ISBN 978-7-03-066724-3, 2020 (in Chinese).

Shan, R. L., Bai, Y., Sui, S. M., Yang, H., and Duan, J. M.: Experimental research on mechanical characteristics of freshwater ice under triaxial compression, Journal of basic science and engineering, 26, 901-917, https://doi.org/10.6052/0459-1879-16-364, 2018 (in Chinese).

Shugar, D. H., Jacquemart, M., Shean, D., Bhushan, S., Upadhyay, K., Sattar, A., Schwanghart, W., McBride, S., Van Wyk 625   de Vries, M., Mergili, M., Emmer, A., Deschamps-Berger, C., McDonnell, M., Bhambri, R., Allen, S., Berthier, E., Car-rivick, J. L., Clague, J. J., Dokukin, D., Dunning, S. A., Frey, F., Gascoin, S., Haritashya, U. K., Huggel, C., Kääb, A., Kargel, J. S., Kavanaugh, J. L., Lacroix, P., Petley, D., Rupper, S., Azam, M. F., Cook, S. J., Dimri, A. P., Eriksson, M., Farinotti, D., Fiddes, J., Gnyawali, K. R., Harrison, S., Jha, M., Koppes, M., Kumar, A., Leinss, S., Majeed, U., Mal, S., Muhuri, A., Noetzli, J., Paul, F., Rashid, I., Sain, K., Steiner, J., Ugalde, F., Watson, C. S., and Westoby, M. J.: A massive 630   rock and ice avalanche caused the 2021 disaster at Chamoli, Indian Himalaya, Science, 373, 300-306, https://doi.org/10.1126/science.abh4455, 2021.

Smith, J. S.: Scaled geotechnical centrifuge modelling of gelifluction, PhD thesis, Cardiff University, Cardiff, The United Kingdom, 442 pp, 2004.

Su, Z. Z., Ma, Y. G., Tan, X. J., Zhang, C. X., Zhou, Y., Ma, X., and Zhang, D. F.: Experimental and theoretical study of the 635   shear strength of ice-rock interface, Cold Regions Science and Technology, 218, 104076, https://doi.org/10.1016/j.coldregions.2023.104076, 2024.

Tian, L. D., Yao, T. D., Gao, Y., Thompson, L., Thompson, E. M., Muhammad, S., Zong, J. B., Wang, C., Jin, S. Q., and Li, Z.G.: Two glaciers collapse in western Ti-bet, Journal of Glaciology, 63, 194-197, https://doi.org/10.1017/jog.2016.122, 2017.

640 Tan, F. L., Hu, X. L., Zhang, Y. M., He, C. C., and Zhang, H.: Study of progres-sive failure processes and stabilities of different types of landslides, Rock and Soil Mechanics, 37, 597-606, https://doi.org/10.16285/j.rsm.2016.S2.075, 2016 (in Chinese).

Tang, M. G., Xu, Q., Deng, W. F., Chen, X., Zhou, J., and Zhao, H. L.: Degradation law of mechanical properties of typical rock in Sichuan-Tibet Traffic Corridor under freeze-thaw and unloading conditions, Earth Science, 47, 1917-1931, https://doi: 10.3799/dqkx.2021.260, 2022 (in Chinese).

Tang, M. G., Xu, Q., Wang, L. N., Zhao, H. L., Wu, G. J., Zhou, J., Li, G., Cai, W. J., and Chen X.: Hidden dangers of ice avalanches and glacier lake outburst floods on the Tibetan Plateau: identification, inventory, and distribution, Landslides, 20, 1-19, https://doi.org/10.1007/s10346-023-02125-4, 2023.

Ting, J. M., Torrence, M. R., and Ladd, C. C.: Mechanisms of strength for frozen sand, Journal of Geotechnical Engineering, 109, 1286-1302, https://doi.org/10.1061/(ASCE)0733-9410(1983)109:10(1286), 1983.

Vivian, R.: The nature of the ice–rock interface: The results of investigation on 20, 000 m² of the rock bed of temperate glaciers, Journal of Glaciology, 25, 267-277, https://doi.org/10.1017/S0022143000010480, 1980.

Wang, T., Jia, H. L., Sun, Q., Lu, T., Tang, L. Y., and Shen, Y.: Pressure melting of pore ice in frozen rock under compression, Cold Regions Science and Technology, 210, 103856, https://doi.org/10.1016/j.coldregions.2023.103856, 2023.

655 Westerveld, B.: Ice-concrete bond analysis: Characterisation of ice adhesion strength in ice-structure interaction, Master thesis, Delft University of Technology, Delft, Netherlands, 103 pp, 2020.

Wei, M. D., Zhang, L. M., and Jiang, R. C.: A conceptual model for evaluating the stability of high-altitude ice-rich slopes through coupled thermo-hydro-mechanical simulation, Engineering Geology, 334, 107514, https://doi.org/10.1016/j.enggeo.2024.107514, 2024.

660 Wilson, C. J. L., Peternell, M., Hunter, N. J. R., and Luzin, V.: Deformation of polycrys-talline D₂O ice: Its sensitivity to temperature and strain-rate as an analogue for terrestrial ice, Earth and Planetary Science Letters, 532, 115999, https://doi.org/10.1016/j.epsl.2019.115999, 2022.

Work, A., and Lian, Y. S.: A critical review of the measurement of ice adhesion to solid substrates, Progress in Aerospace Sciences, 98, 1-26, https://doi.org/10.1016/j.paerosci.2018.03.001, 2018.

665 Xu, L. M., Wang, T. Z., Qi, D. Q., Yu, C. H., and Gu, L.: Study on geotechnical shear band localization retrospect and prospect, Chinese Quarterly of Mechanics, 25, 484-489, https://doi.org/10.15959/j.cnki.0254-0053.2004.04.008, 2004 (in Chinese).

Xu, H. Y., Lai, Y. M., Yu, W. B., Xu, X. T., and Chang, X. X.: Experimental research on triaxial strength of polycrystalline ice, Journal of glaciology and geocryology, 33, 1120-1126, https://doi.org/10.7522/j.issn.1000-0240.2011.0154, 2011 (in 670 Chinese).

Zhang, D. M.: Theoretical and experimental research on deformation localization and instability of rock, PhD thesis, Chongqing University, Chongqing, China, 188 pp, 2004 (in Chinese).

Zhang, T. G., Wang, W. C., Shen, Z. H., and An, B. S.: Increasing frequency and de-structiveness of glacier-related slope failures under global warming, Science Bul-letin, 69, 30-33, https://doi.org/ 10.1016/j.scib.2023.09.042, 2024.

675   Zhang, Y. J., Zhang, Y. H., Guo, R. Z., and Cui B.: Method for testing shear and tensile strengths of freshwater/seawater ice, Water, 14, 1363, https://doi.org/10.3390/w14091363, 2022.

Zhao, C. X., Yang, W., Westoby, M., An, B. S., Wu, G. J., Wang, W. C., Wang, Z. Y., and Wang, Y. J.: Dunning Stuart. Brief communication: An approximately 50 Mm3 ice–rock avalanche on 22 March 2021 in the Sedongpu valley, southeastern Ti-betan Plateau, The Cryosphere, 16, 1333-1340, https://doi.org/10.5194/tc-16-1333-2022, 2022.

680